THE OFFICIAL MAGAZINE OF THE OCEANOGRAPHY SOCIETY

Oceanography

CITATION

Wdowinski, S., S.-H. Hong, A. Mulcan, and B. Brisco. 2013. Remote-sensing monitoring of tide propagation through coastal wetlands. *Oceanography* 26(3):64–69, http://dx.doi.org/10.5670/oceanog.2013.46.

DOI

http://dx.doi.org/10.5670/oceanog.2013.46

Remote-Sensing Monitoring of Tide Propagation Through Coastal Wetlands

BY SHIMON WDOWINSKI, SANG-HOON HONG, AMANDA MULCAN, AND BRIAN BRISCO

ABSTRACT. Tide propagation through coastal wetlands is a complex phenomenon affected by vegetation, channels, and tidal conditions. Generally, tidal flow is studied using stage (water level) observations, which provide good temporal resolution, but they are acquired in limited locations. Here, a remote-sensing technique, wetland InSAR (interferometric synthetic aperture radar), is used to detect tidal flow in vegetated coastal environments over broad spatial scales. The technique is applied to data sets acquired by three radar satellites over the western Everglades in south Florida. Interferometric analysis of the data shows that the greatest water-level changes occur along tidal channels, reflecting a high velocity gradient between fast horizontal flow in the channel and the slow flow propagation through the vegetation. The high-resolution observations indicate that the tidal flushing zone extends 2–3 km on both sides of tidal channels and can extend 3–4 km inland from the end of the channel. The InSAR observations can also serve as quantitative constraints for detailed coastal wetland flow models.

INTRODUCTION

Coastal wetlands, including mangrove forests and saltwater marshes, are considered among the most valuable ecosystems on Earth, yet their existence is presently being threatened by climate change (sea level rise) and human interference (e.g., infrastructure development). These fragile ecosystems depend on continuous water and nutrient replenishment by ocean tidal flow and often also by freshwater flow. Although ocean tides are well known and forecasted, tidal flow movements through coastal wetlands are poorly known because vegetation resists the flow and delays both inland and seaward flow at rising and subsiding tide conditions, respectively. Thus far, most observations on tide propagation through coastal wetlands have been obtained from stage (water level) measurements within the vegetated tidal zone (e.g., Mazda et al., 1995; Holtermann et al., 2009). These stage measurements can produce high temporal resolution observations, but they are acquired at a limited number of measurement points.

Remote-sensing observations, in particular, satellite imagery, serve as very useful tools for characterizing spatial phenomena, such as land cover and its changes over time. Optical and synthetic aperture radar imagery have been widely used to detect and monitor coastal wetlands, mainly for vegetation classification and estimating biological parameters, such as aboveground biomass (Simard et al., 2006; Schalles et al., 2013, in this issue). However, most of these remote-sensing techniques cannot detect water levels in wetlands, as the water is often beneath the vegetation cover.

Interferometric synthetic aperture radar (InSAR) is a very reliable remote-sensing technique for monitoring changes in Earth's solid and aquatic surfaces (Box 1). Wetland InSAR is a relatively new application of this technique that detects water-level changes in aquatic environments with emergent vegetation (Wdowinski et al., 2004, 2008). Obtaining coherent phase observations (Box 1) in both aquatic and vegetated environments over several days was not thought possible because short-term processes such as wind or water flow can change the shape of the scattering surface. However, the fact that coherent InSAR observations can be obtained in wetlands indicates that they are stable for SAR scattering and can maintain phase over weeks and months (Kim et al., 2013). Indeed, the method has been successfully applied to study wetland hydrology in the Everglades (Wdowinski et al., 2004, 2008; Hong et al., 2010), in Louisiana (Kim et al., 2009; Kwoun and Lu, 2009), and at other locations (e.g., Gondwe et al., 2010).

In this study, we use high spatial resolution InSAR observations to detect surface water-level changes in response to ocean tide propagation through the coastal Everglades' mangrove forests. The observations show that the highest rate of water-level changes occurs near tidal channels, reflecting a high velocity gradient between fast horizontal flow

BOX 1 | SYNTHETIC APERTURE RADAR

Synthetic aperture radar (SAR) is an active remote-sensing technique that transmits and receives radar signals over a wide swath (15–400 km) with spatial pixel resolution of 1–100 m depending on satellite acquisition parameters. It measures two independent observation types—backscatter amplitude and phase. Backscatter amplitude, which is often presented as gray-scale images of the surface, is very sensitive to surface dielectric properties, surface inclination toward the satellite, and wave direction in the ocean. Amplitude images are widely used for studying surface classification, soil moisture content, ocean waves, and many other applications (e.g., Cloude and Pottier, 1996).

The second observation type, backscatter phase, measures the fraction of the radar wavelength that returns to the satellite's antenna. It is mainly sensitive to the range or distance between the surface and the satellite, but also to atmospheric conditions and changes in the surface dielectric properties. Phase data are mostly used in interferometric calculations (InSAR) for detecting subcentimeter-level displacements of the surface (Burgmann et al., 2000). The method compares pixel-by-pixel SAR phase observations of the same area acquired at different times from roughly the same location in space (up to 4 km deviation between repeated orbits) to produce high-spatial-resolution surface change maps.

The results of SAR interferometric processing are detailed colorful maps, termed interferograms, which show phase changes occurring between two acquisition times. These phase changes are referred to as "fringes" and represent mostly line-of-sight changes between Earth's surface and the satellite, which can include both vertical and horizontal surface movements. However, some of the fringes represent changes in atmospheric moisture content between the two acquisition times, because atmospheric moisture delays the transmission of the SAR signal to and from the satellite.

A quality measure of an interferogram is termed coherence, which calculates spatial consistency of the calculated phase. High interferometric coherence is reflected in continuous fringe patterns, whereas low coherence appears as a fuzzy phase pattern. Interferograms are widely used in studies of earthquake-induced crustal deformation, magmatic activity, water-table fluctuations, and glacier movements (Wdowinski and Eriksson, 2009).

Transforming an interferogram's phase measurements to water-level changes requires an advanced spatial analysis of the phase information and knowledge of the sensor's wavelength and acquisition geometry. The advanced spatial analysis, termed unwrapping, expands the range of the observed phase, which is wrapped in the range $0–2\pi$, to a much larger range (e.g., $0–8\pi$), depending on the phase pattern and distribution. Then, the unwrapped phase is multiplied by half of the sensor's wavelength and a geometric factor based on the satellite's viewing angle of Earth's surface. More details on phase transformation to water-level change can be found in Wdowinski et al. (2008).

in the channel and slow flow propagation through the mangrove forest. The high-resolution observations enable us to characterize the extent of the tidal flushing zone and provide quantitative constraints for detailed coastal wetland flow models.

STUDY AREA

Our study area consists of coastal wetlands located within the boundaries of the Everglades National Park (ENP), southern Florida (Figure 1). This area has been intensively studied by the Florida Coastal Everglades Long Term Ecological Research (FCE LTER) project over the past two decades. We focus on the western side of ENP, which consists of a wide zone of coastal wetlands, extending up to 35 km inland from the Gulf of Mexico shoreline.

The vegetation in the study area includes both freshwater swamps and saltwater mangroves, with a variety of vegetation types comprising a very rich ecosystem (Figure 1a). The freshwater swamps consist mainly of sawgrass (herbaceous vegetation) and islands of hardwood hammock (tree islands). In between the freshwater swamps and the saltwater mangroves there is a transition zone with mixed vegetation, often termed prairies. The saltwater mangrove forests contain trees of variable height. Short mangroves are found in many locations around the park (Figure 1b), whereas tall mangrove trees (> 15 m high) are located mainly in the southwestern corner of the park (Simard et al., 2006) in areas dissected by numerous tidal channels (Figure 1c).

RESULTS

We used data sets acquired by three satellites to detect water-level changes in the Everglades tidal zone (Figure 2). The satellites operate at three different radar wavelengths that have different sensitivities to the vegetation. Short-wavelength radar signals tend to interact mainly with upper sections of the vegetation, whereas longer-wavelength signals can penetrate the vegetation and interact with tree trunks and the ground beneath the vegetation. We used L-band (24 cm), C-band (5.6 cm), and X-band (3.1 cm wavelength) SAR data that were acquired by the Japanese Advanced Land Observing Satellite (ALOS), the Canadian Radarsat-2 (RSAT-2) satellite, and the German TerraSAR-X (TSX) satellite, respectively. We processed the data using the software package ROI_PAC (Buckley et al., 2000), which generates interferograms from pairs of the same sensor data.

Figure 2 shows the interferograms. They provide spatially detailed information on water-level changes with pixel resolution of 10–20 m. The water level changes occur between the two satellites' acquisition times, which vary according to each satellite's repeat orbit period or its multiples (ALOS – 46 days; RSAT-2 – 24 days; TSX – 11 days). Because the time spans between data acquisitions are not synchronized with tide levels, the interferograms can detect differential water-level changes in the tidal zone.

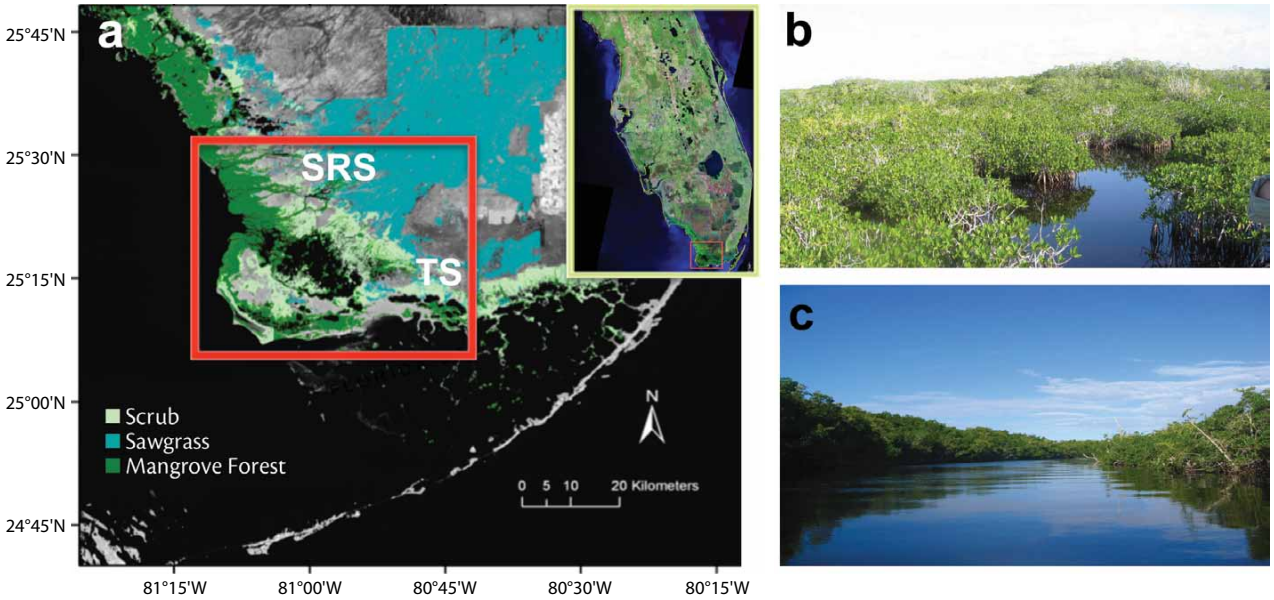

Figure 1. Location and morphology of coastal wetlands in the southern Florida Everglades. (a) Vegetation map of Everglades National Park showing mangrove forest distribution mainly along the west coast but also scattered along the southern coast. *Florida Coastal Everglades Long Term Ecological Research; http://fcelter.fiu.edu.* (b) Dwarf mangrove morphology in Taylor Sough. (c) Tall mangrove forests along tidal channels in Shark Valley Slough. TS = Taylor Slough. SRS = Shark River Slough.

If they were synchronized, water-level changes between acquisitions at similar tide level conditions would be minimal and undetectable by InSAR.

In the L-band image (Figure 2b), the two fringes that follow geographic features and most likely reflect water-level changes are: (1) a linear roughly north-south oriented fringe located east of Tarpon Bay and (2) a rounded fringe surrounding Tarpon Bay. The location and orientation of the linear fringe follows the transition zone between fresh- and saltwater vegetation, reflecting tide-induced water-level changes in the saltwater marshes. The rounded fringe around Tarpon Bay has a more pronounced appearance in the other interferograms and is discussed in detailed below.

The RSAT-2 interferogram (Figure 2c) shows a more complex fringe pattern that can be characterized by the following three zones: (1) low fringe gradient in the northeastern corner, (2) incoherent phase (fuzzy pattern) in the southwest corner, and (3) a wide northwest-southeast belt with high fringe gradient. The low fringe gradient in the northeast corner occurs in the freshwater wetlands. It reflects slow changes in freshwater sheetflow and possibly some atmospheric signals. The incoherent signal in the southwest corner occurs over tall mangrove vegetation, which causes unstable scattering in the C-band SAR signal. The high fringe gradient in the transition zone occurs over variable vegetation types, including intermediate and short mangrove forests.

The fringes that surround Tarpon Bay and other water bodies reflect water-level changes. The fringes result from the high contrast between fast flow in the channel and slow flow through the saltwater vegetation. When we examined the fringe pattern along Tarpon Bay in more detail, we found that each phase change corresponded to about 4 cm of elevation change. Thus, the total change along Tarpon Bay is 12 cm. A comparison between the space-based InSAR and ground-based stage (water level) measurements indicates that both techniques agree within 1–3 cm, indicating the accuracy of the InSAR measurements. It is interesting to note that the InSAR-detected slope is very small, ~ 5×10^{-5}, which is less than 1/100 of a percent. Such small slope cannot be detected from the

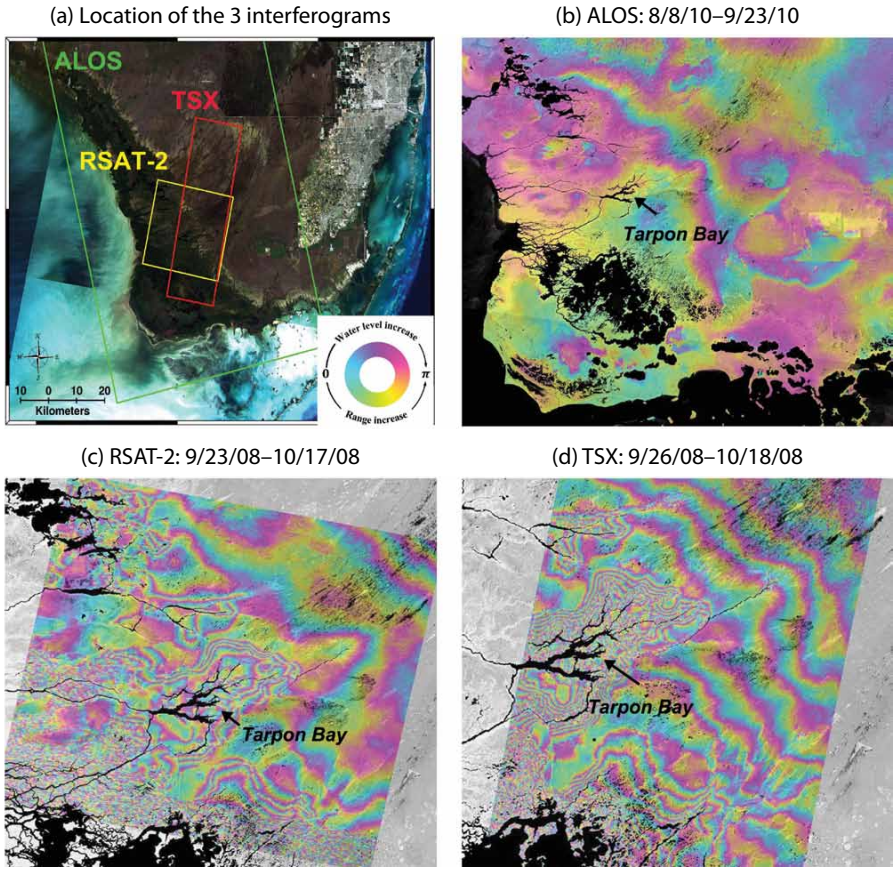

Figure 2. (a) Google Earth composite satellite image showing the areas of the three interferograms used in the study area. (b) Advanced Land Observing Satellite (ALOS) interferogram showing coherent fringe along the transition between fresh- and saltwater vegetation and partial fringe along the tidal channels. (c) Radarsat-2 (RSAT-2) interferogram showing short-wavelength fringes surrounding tidal channels in the mangrove forest area. (d) TerraSAR-X interferogram showing similar fringe patterns around the tidal channels. The different number of fringes in each interferogram reflects sensor sensitivity for detecting surface changes. Each ALOS (L-band) fringe reflects 15 cm of water level change, RSAT-2 (C-band) 4 cm, and TerraSAR-X (X-band) 2 cm.

Shimon Wdowinski *(shimonw@rsmas.miami.edu) is Research Associate Professor, Division of Marine Geology and Geophysics, University of Miami, Miami, FL, USA.* **Sang-Hoon Hong** *was Postdoctoral Scientist, Division of Marine Geology and Geophysics, University of Miami, Miami, FL, USA, and is now at the Satellite Information Research Center, Korea Aerospace Research Institute, Republic of Korea.* **Amanda Mulcan** *is a graduate student in the Division of Marine Geology and Geophysics, University of Miami, Miami, FL, USA.* **Brian Brisco** *is a scientist in the Earth Observation and GeoSolutions Division, Canada Centre for Remote Sensing, Natural Resources Canada, Ottawa, Ontario, Canada.*

ground, but can easily be measured by InSAR from space.

The X-band TSX interferogram (Figure 2d) covers only part of the area shown in the RSAT-2 interferogram (Figure 2c), but again, it shows a high fringe gradient surrounding Tarpon Bay. However, the TSX interferogram has more fringe cycles compared to the RSAT-2 (six vs. three cycles) for the same amount of water-level change (12 cm). This reflects the shorter wavelength of the TSX radar signal (3.1 cm) compared to the RSAT-2 signal (5.6 cm). The phase information can be translated to water-level changes based on the SAR wavelength and the acquisition geometry; the measured change is 2 cm per phase cycle for TSX and 4 cm for RSAT-2. A second difference between these images is that the fringe order is reversed (blue-yellow-red with distance to the bay in the TSX vs. blue-red-yellow in the RSAT-2). This reversal indicates that the TSX interferogram recorded a negative water-level change in which the smallest water-level change occurs in the bay and the slopes are directed toward the bay and not outward as in the RSAT-2 interferogram.

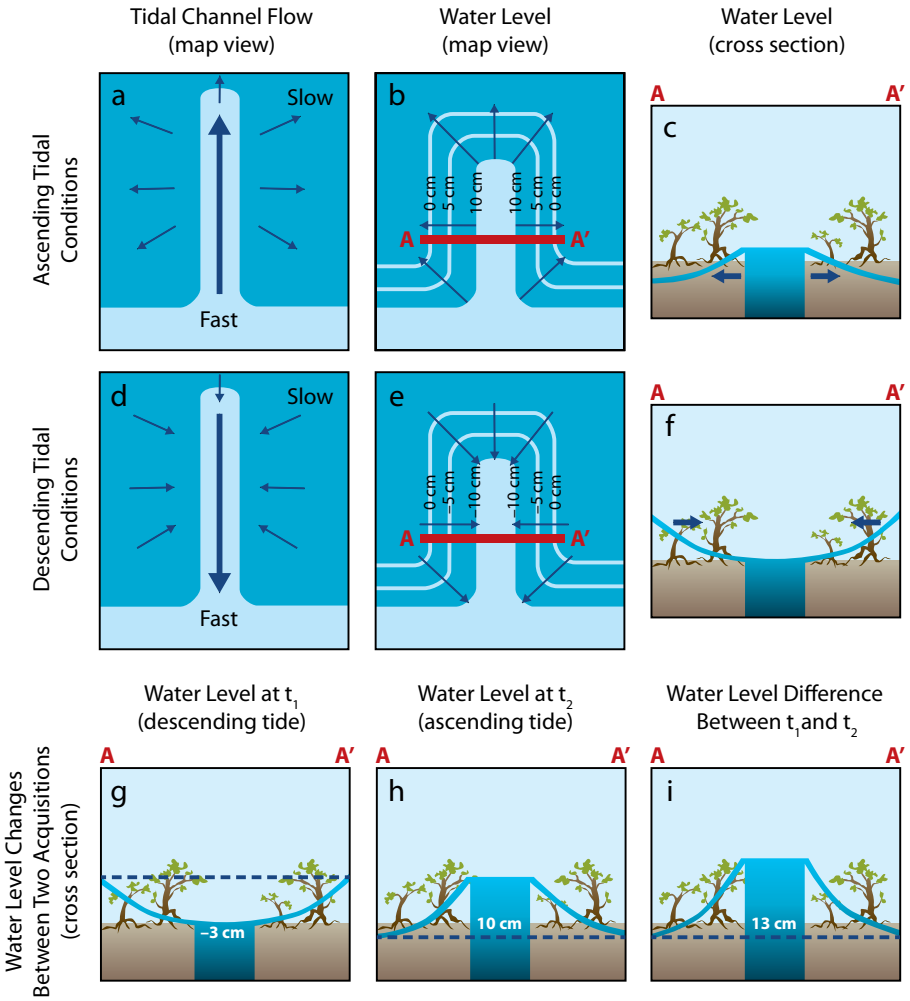

Figure 3. Schematic illustration explaining the relationship between water-level changes along tidal channels and tidal flow dynamics in mangrove forests. (a) Ascending tidal conditions: tidal inflow is fast in the channel (light blue) but slow in the mangrove forest (dark blue) due to the vegetation's resistance to the flow. (b) Water level is highest in the channel and decreases with distance from the channel. (c) Cross section of water level across the channel. (d) Descending tidal conditions: fast tidal outflow through the channel but slow tidal flow through the vegetated area. (e) Water level is lowest in the channel and increases with distance from the channel. (f) Cross section of water level across the channel. (g and h) Cross sections of water levels during two SAR data acquisition times (t_1 and t_2). Water levels are measured with respect to the far field. (i) Water-level changes, observed by InSAR, between the two acquisition times.

Water-Level Changes and Tidal Flow Dynamics

The three interferograms presented in Figure 2 detected variable water-level changes throughout the tidal zone, with the largest changes along tidal channels. These differences, which can be related to tidal flow dynamics, are summarized in Figure 3.

In a channeled wetland environment, as occurs in the western Everglades, the tide propagates quickly along channels and more slowly in vegetated areas because vegetation is highly resistant to flow. During ascending tidal conditions, the tide moves inland through the channel, resulting in higher water levels as compared to its vegetated surroundings (Figure 3a). The water then propagates slowly through the vegetation. As a result, water levels are highest in the channel and decrease with distance from it (Figure 3b,c). During descending tidal conditions, water levels subside rapidly in the channel, resulting in a reversal, with lower water levels closer to the channel (Figure 3d,e,f).

Phase changes detected by InSAR reflect water-level changes, which occurred due to differences in tidal elevation between the two acquisition times (11, 24, and 46 days for the TSX, RSAT-2, and ALOS, respectively). We illustrate this in Figure 3g and h, which shows one scenario of ascending and the other of descending tide conditions. Figure 3i shows the elevation change

between the two acquisition snapshots, which is similar to the water-level changes detected across Tarpon Bay.

DISCUSSION AND APPLICATIONS

The wetland InSAR observations acquired over the western Everglades provide a spatially detailed picture of tidally induced water-level changes that cannot be detected by any terrestrial measurement technique. The InSAR measurements are sensitive to small changes in water levels, on the order of a few centimeters, that occur over distances of several kilometers. The method can detect minute changes in water surface slope, as small as a hundredth of a percent. The high sensitivity of the method enables us to detect lateral changes in tidal flow propagation through coastal wetlands. In this study, we found that the highest water-level changes occur along tidal channels, reflecting the slow response of vegetated areas to rapid water-level changes within the tidal channel.

We can also use the interferograms to evaluate tidal flushing, as a high fringe gradient along the tidal channel is a good indicator of the tidal flushing zone's width. In this case, we estimate that the zone is 2–3 km wide, depending on tide conditions. This zone of high fringe gradient is also a good indicator of the inland propagation of tidal flow, which can vary seasonally due to changes in the hydraulic head in the freshwater wetlands. Both the RSAT-2 and the TSX interferograms show that the tidal flushing zone extends 4–5 km east of Tarpon Bay.

Finally, the interferograms provide a quantitative measure of water-level changes that can be converted to detailed maps of water-level changes. Such maps can serve as useful constraints for quantitative tidal flow models. We plan to conduct such detailed flow models as part of the FCE LTER project.

ACKNOWLEDGEMENTS

We are thankful for comments and suggestions from Guest Editor Merryl Alber and two anonymous reviewers. This work was enabled by the TSX science proposal (HYD0029) and the SOAR project from CSA for access to the TerraSAR-X and the Radarsat-1/2 data. We also thank the Japan Aerospace Exploration Agency (JAXA) and the Alaska Satellite Facility (ASF) for access to ALOS data. We thank the National Center for Airborne Laser Mapping for the photo on the opening page of this article. The research was supported by NASA Cooperative Agreement NNX10AQ13A (WaterSCAPES: Science of Coupled Aquatic Processes in Ecosystems from Space) and by the National Science Foundation through the Florida Coastal Everglades Long Term Ecological Research program under grant DEB-1237517. Additional support for this research was provided by the CSA through the RCM/CCD project and the Remote Sensing Science Program at CCRS.

REFERENCES

Buckley, S.M., P.A. Rossen, and P. Persaud. 2000. ROI_PAC documentation: Repeat orbit interferometry package. Available online at: http://www.earth.ox.ac.uk/~timw/roi_pac/ROI_PAC_doc.pdf (accessed July 11, 2013).

Burgmann, R., Rosne, P.A. and E.J. Fielding. 2000. Synthetic aperture radar interferometry to measure Earth's surface topography and its deformation. *Annual Review of Earth and Planetary Sciences* 28:169–209, http://dx.doi.org/10.1146/annurev.earth.28.1.169.

Cloude, S.R., and E. Pottier. 1996. A review of target decomposition theorems in radar polarimetry. *IEEE Transactions on Geoscience and Remote Sensing* 34:498–518, http://dx.doi.org/10.1109/36.485127.

Gondwe, B.R.N., S.H. Hong, S. Wdowinski, and P. Bauer-Gottwein. 2010. Hydrologic dynamics of the ground-water-dependent Sian Ka'an Wetlands, Mexico, derived from InSAR and SAR data. *Wetlands* 30(1):1–13, http://dx.doi.org/10.1007/s13157-009-0016-z.

Holtermann, P., H. Burchard, and T. Jennerjahn. 2009. Hydrodynamics of the Segara Anakan lagoon. *Regional Environmental Change* 9(4):245–258, http://dx.doi.org/10.1007/s10113-008-0075-3.

Hong, S.H., S. Wdowinski, and S.W. Kim. 2010. Evaluation of TerraSAR-X observations for wetland InSAR application. *IEEE Transactions on Geoscience and Remote Sensing* 48(2):864–873, http://dx.doi.org/10.1109/TGRS.2009.2026895.

Kim, J.W., Z. Lu, H. Lee, C.K. Shum, C.M. Swarzenski, T.W. Doyle, and S.H. Baek. 2009. Integrated analysis of PALSAR/Radarsat-1 InSAR and ENVISAT altimeter data for mapping of absolute water level changes in Louisiana wetlands. *Remote Sensing of Environment* 113(11):2,356–2,365, http://dx.doi.org/10.1016/j.rse.2009.06.014.

Kim, S.-W., S. Wdowinski, A. Amelung, T.H. Dixon, and J.-S. Won. 2013. Interferometric coherence analysis of the Everglades wetlands, South Florida. *IEEE Transactions on Geoscience and Remote Sensing* 51:1–15, http://dx.doi.org/10.1109/TGRS.2012.2231418.

Kwoun, O.I., and Z. Lu. 2009. Multi-temporal RADARSAT-1 and ERS backscattering signatures of coastal wetlands in southeastern Louisiana. *Photogrammetric Engineering and Remote Sensing* 75(5):607–617.

Mazda, Y., N. Kanazawa, and E. Wolanski. 1995. Tidal asymmetry in mangrove creeks. *Hydrobiologia* 295:51–58, http://dx.doi.org/10.1007/BF00029110.

Schalles, J.F., C.M. Hladik, A.A. Lynes, and S.C. Pennings. 2013. Landscape estimates of habitat types, plant biomass, and invertebrate densities in a Georgia salt marsh. *Oceanography* 26(3):88–97, http://dx.doi.org/10.5670/oceanog.2013.50.

Simard, M., K.Q. Zhang, V.H. Rivera-Monroy, M.S. Ross, P.L. Ruiz, E. Castaneda-Moya, R.R. Twilley, and E. Rodriguez. 2006. Mapping height and biomass of mangrove forests in Everglades National Park with SRTM elevation data. *Photogrammetric Engineering and Remote Sensing* 72(3):299–311.

Wdowinski, S., F. Amelung, F. Miralles-Wilhelm, T.H. Dixon, and R. Carande. 2004. Space-based measurements of sheet-flow characteristics in the Everglades wetland, Florida. *Geophysical Research Letters* 31, L15503, http://dx.doi.org/10.1029/2004GL020383.

Wdowinski, S., and S. Eriksson. 2009. Geodesy in the 21st Century. *Eos, Transactions, American Geophysical Union* 90(18):153–155, http://dx.doi.org/10.1029/2009EO180001.

Wdowinski, S., S.W. Kim, F. Amelung, T.H. Dixon, F. Miralles-Wilhelm, and R. Sonenshein. 2008. Space-based detection of wetlands' surface water level changes from L-band SAR interferometry. *Remote Sensing of Environment* 112(3):681–696, http://dx.doi.org/10.1016/j.rse.2007.06.008.